Check for updates

Heart failure causally affects the brain cortical structure: a Mendelian randomization study

Tianjiao Meng[1†], Qinwen Fei[2†], Jingying Zhu[3†], Jiayi Gu[4], Weiyu Li[5,6], Xianhong Wu[6], Gonghua Pan[6], Tian Lv[1]* and Shiqin Chen[6]*

[1]Department of Neurology, Zhuji Affiliated Hospital of Wenzhou Medical University, Zhuji, China, [2]Department of Geriatrics, Zhuji Affiliated Hospital of Wenzhou Medical University, Zhuji, China, [3]Department of Emergency, Taizhou Hospital, Taizhou, China, [4]Wenzhou People's Hospital, Wenzhou, China, [5]The First Clinical Medical Institute of Wenzhou Medical University, Wenzhou Medical University, Wenzhou, China, [6]Department of Neurology, Second People's Hospital of Yuhuan, Yuhuan, China

Background: The effects of heart failure (HF) on cortical brain structure remain unclear. Therefore, the present study aimed to investigate the causal effects of heart failure on cortical structures in the brain using Mendelian randomization (MR) analysis.

Methods: We conducted a two-sample MR analysis utilizing genetically-predicted HF trait, left ventricular ejection fraction (LVEF), and N-terminal prohormone brain natriuretic peptide (NT-proBNP) levels to examine their effects on the cortical surface area (SA) and thickness (TH) across 34 cortical brain regions. Genome-wide association study summary data were extracted from studies by Rasooly (1,266,315 participants) for HF trait, Schmidt (36,548 participants) for LVEF, the SCALLOP consortium (21,758 participants) for NT-proBNP, and the ENIGMA Consortium (51,665 participants) for cortical SA and TH. A series of MR analyses were employed to exclude heterogeneity and pleiotropy, ensuring the stability of the results. Given the exploratory nature of the study, p-values between $1.22E-04$ and 0.05 were considered suggestive of association, and p-values below $1.22E-04$ were defined as statistically significant.

Results: In this study, we found no significant association between HF and cortical TH or SA (all $p > 1.22E-04$). We found that the HF trait and elevated NT-proBNP levels were not associated with cortical SA, but were suggested to decrease cortical TH in the pars orbitalis, lateral orbitofrontal cortex, temporal pole, lingual gyrus, precuneus, and supramarginal gyrus. Reduced LVEF was primarily suggested to decrease cortical SA in the isthmus cingulate gyrus, frontal pole, postcentral gyrus, cuneus, and rostral middle frontal gyrus, as well as TH in the postcentral gyrus. However, it was suggested to causally increase in the SA of the posterior cingulate gyrus and medial orbitofrontal cortex and the TH of the entorhinal cortex and superior temporal gyrus.

Conclusion: We found 15 brain regions potentially affected by HF, which may lead to impairments in cognition, emotion, perception, memory, language, sensory processing, vision, and executive control in HF patients.

KEYWORDS

heart failure, Mendelian randomization, cortical structure, heart-brain axis, left ventricular ejection fraction

1 Introduction

Heart failure (HF) is now widely acknowledged as a systemic clinical syndrome characterized by insufficient cardiac function linked to multiple organ dysfunction and various co-existing conditions (Doehner et al., 2023). HF often affects the brain and other vital organs, leading to structural and functional abnormalities (Havakuk et al., 2017). Research has shown that individuals with HF may experience a range of neurological impairments, including decreased attention, cognitive dysfunction, dementia, stroke, depression, and autonomic nervous system dysfunction, among others (Florea and Cohn, 2014; Villringer and Laufs, 2021; Doehner et al., 2023). Similarly, the concepts of the heart-brain axis and heart-brain syndrome have become widely accepted (Havakuk et al., 2017; Hooghiemstra et al., 2019).

Focusing on the impact of HF on brain structure, Mueller et al. (2020) found that biomarkers of heart failure, such as left ventricular ejection fraction (LVEF) and N-terminal prohormone brain natriuretic peptide (NT-proBNP) levels, were linked to decreased gray matter density across the entirety of the frontomedian cortex, hippocampus, and precuneus. These observations may reflect structural damage to brain regions associated with cognition. In one prior study utilizing magnetic resonance T2 relaxometry, Woo et al. (2009) discovered that HF patients exhibited differences in regions controlling emotional, cognitive, autonomic, and analgesic functions (temporal, parietal, prefrontal, occipital, insular, cingulate, and ventral frontal cortices; anterior thalamus; caudate nuclei; anterior fornix and hippocampus; hypothalamus, raphé magnus, cerebellar cortex, deep nuclei and vermis; corpus callosum, respectively) compared to controls, suggesting abnormalities in emotional, cognitive, autonomic, and pain functions among HF patients. One review summarising a series of studies achieved similar findings (Alosco and Hayes, 2015). However, observational studies are influenced by many confounding factors; for example, patients with HF often have concomitant advanced age, hypertension, obesity, diabetes, and cardiovascular diseases, and the sample sizes of these studies were usually small. Therefore, the current research results have not been fully validated. Mendelian randomization (MR) can overcome these limitations. The MR approach uses genetic variants to evaluate the causal associations between exposure and outcome variables (Sekula et al., 2016). When applied to large datasets, MR analysis could serve as an excellent method for exploring the impact of HF on brain structure.

In the present study, we utilized human genetic data within the MR framework to investigate the impact of HF on the structure of the brain cortex, specifically the cortical surface area (SA) and cortical thickness (TH), measured using magnetic resonance imaging (MRI). Three sets of HF parameters were used to derive the MR estimates: HF trait, LVEF, and NT-proBNP. Overall, this study provides valuable insights into the heart-brain axis.

2 Materials and methods

2.1 Study design

This study examined the causal relationships between HF and cortical structures using a two-sample MR approach. Figure 1 presents an overview of the study design.

To ensure a reliable MR method, three fundamental assumptions must be satisfied: first, the genetic instruments should be strongly associated with the exposure; second, the genetic instruments should not be linked to confounding factors; and third, the genetic instruments should only influence the outcomes through the exposures (Richmond and Davey Smith, 2022). The independence of the horizontal pleiotropy, which encompasses the second and third assumptions, can be effectively evaluated using diverse statistical methods (Emdin et al., 2017).

2.2 Data sources for HF, LVEF and NT-proBNP

HF data were obtained from a large-scale meta-analysis of genome-wide association studies (GWAS) conducted by Rasooly et al. (2023), encompassing over 90,000 cases and 1 million control individuals of European ancestry. Detailed cohort information is provided in Supplementary Table S1. In their findings, the researchers identified 39 genome-wide significant HF risk variants, including 18 that were previously unreported. Summary statistics related to LVEF were extracted from a study by Schmidt et al. (2023), who conducted a GWAS on 16 cardiac magnetic resonance (CMR) traits measured in up to 36,548 UK Biobank subjects using a thoroughly validated deep-learning approach. Genetic data for NT-pro_BNP were acquired through a GWAS conducted by the SCALLOP consortium (Folkersen et al., 2020), comprising 13 cohorts, totaling 21,758 individuals of European descent; detailed cohort information is provided in Supplementary Table S2.

In summary, utilizing the largest and up-to-date accessible GWAS datasets focused on HF, LVEF, and NT-proBNP, we investigated the potential causal relationships between these HF-related traits and cortical brain structure.

2.3 Data source for brain cortex SA and cortex TH

GWAS data related to brain cortical structures were acquired from the ENIGMA Consortium (Grasby et al., 2020). Brain cortical TH and SA measurements were conducted using MRI on 51,665 individuals, predominantly (~94%) of European descent, across 60 cohorts worldwide. In our study, we specifically employed meta-results derived exclusively from participants of European ancestry, and detailed information about the cohorts is provided in Supplementary Table S3. The 34 cortical regions were delineated based on the Desikan-Killiany atlas, which establishes coarse partitions for the cortex. Regional boundaries were determined in accordance with the gyral anatomy, and were specifically identified between the depths of the sulci (Desikan et al., 2006). Subsequently, these regions were averaged across both hemispheres.

2.4 Selection of genetic instruments

To investigate the causal relationship between HF and the cortical structure of the brain, we employed three distinct sets of genetic

FIGURE 1
Study design schematic.
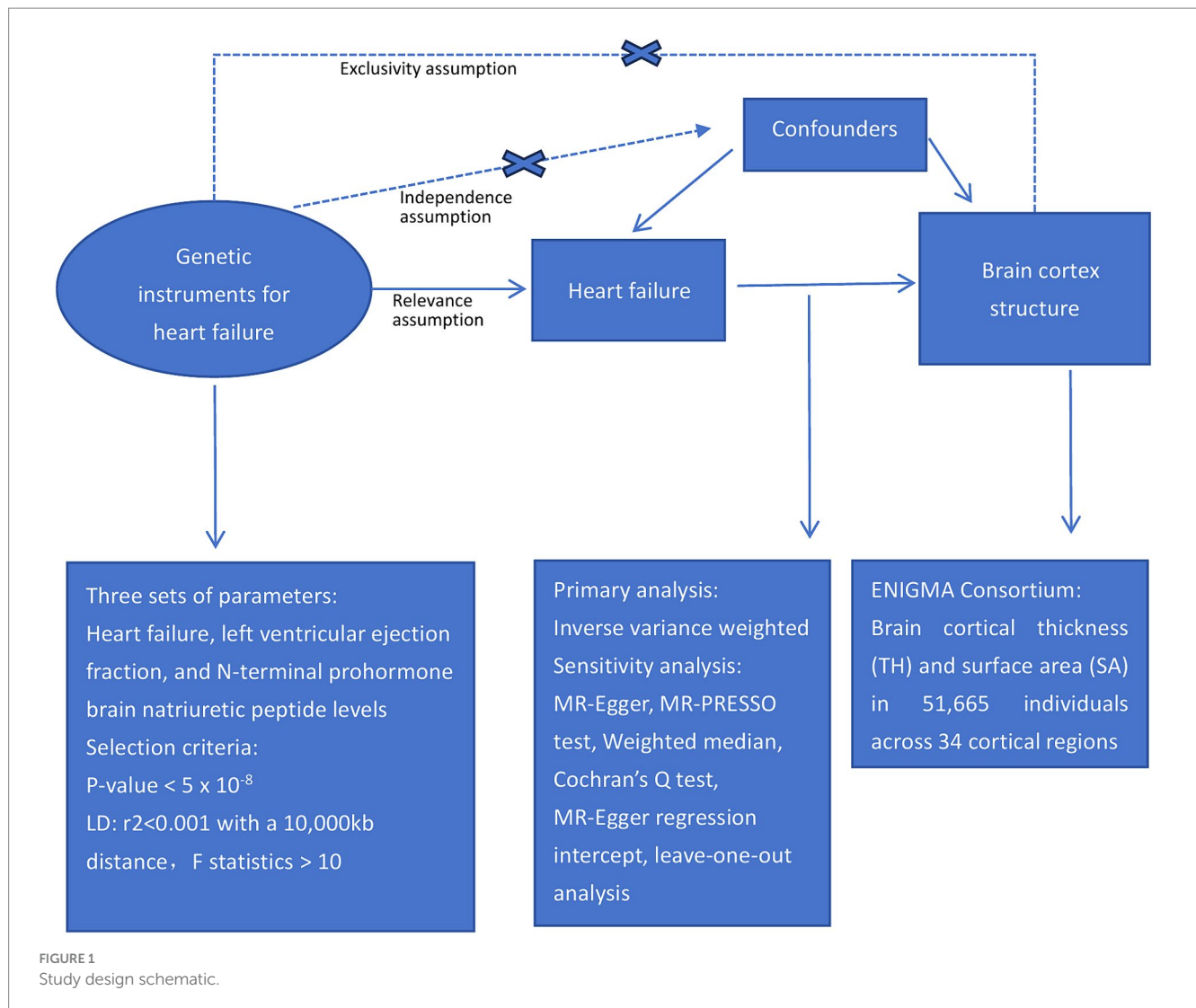
instruments that signify different facets of heart pathophysiology. Genetic instruments were selected based on the following criteria:

i) A GWAS-correlated *p*-value <5E−08.

ii) Linkage disequilibrium [LD] r2 < 0.001, within a 10,000 kb distance to enhance the independence of single-nucleotide polymorphisms (SNPs).

iii) To ensure result precision and minimize the impact of weak instruments, F statistics (beta²/se²) were calculated for all SNPs to assess their statistical strength.

iv) Exposure SNPs showing a significant association (*p* < 5E−08) with the outcome were subsequently eliminated.

v) Harmonization was performed to align the alleles of the exposure and outcome SNPs. Palindromic SNPs with incompatible alleles, such as A/G vs. A/C, were also removed.

Overall, 36 index SNPs representing HF (Supplementary Table S4), and 14 index SNPs representing LVEF (Supplementary Table S5) were identified. One index SNP representing NT-pro_BNP was found at a threshold of *p* < 5E−08. However, relying on a single SNP may not fully capture the complexity of the trait (Boehm and Zhou, 2022). Using a looser threshold of p < 5E−06 (Ference et al., 2015; Li et al., 2022), 12

index SNPs for NT-pro_BNP were identified (Supplementary Table S6). With a lowered significance threshold, F statistics were used to assess the potential for weak instrument bias, and all SNPs demonstrated F statistics >10, indicating no bias.

Notably, the lack of overlap among the 36 HF-SNPs in Supplementary Table S4, 14 LVEF-SNPs in Supplementary Table S5, and 12 BNP-SNPs in Supplementary Table S6 indicated the specificity of these instruments.

2.5 MR analysis

We employed the inverse variance weighted (IVW) method in the primary analysis to investigate the relationships between heart failure and brain cortical structure. The IVW method is commonly used to estimate causal associations. Results were considered indicative of a suggestive causal relationship between heart failure and brain cortical structures at *p* < 0.05. This method assumes the validity of all genetic variants, making it a valuable approach for MR estimation, despite its susceptibility to pleiotropic bias (Bowden et al., 2015).

2.6 Sensitivity analysis

When more than three SNPs were available, sensitivity analyses were conducted using various MR approaches. These included the weighted median, MR-Egger regression, and Mendelian randomization-pleiotropy residual sum and outlier (MR-PRESSO) methods, each of which utilizes distinct assumptions that influence the statistical power. The weighted median approach provided consistent estimates, ensuring reliability when more than half of the weights were derived from valid SNPs (Verbanck et al., 2018). In contrast, MR-Egger analysis is capable of adjusting for pleiotropy and making causal inferences even when all genetic variants exhibit pleiotropic effects (Burgess and Thompson, 2017). Cochran's Q test was used to assess heterogeneity (Greco et al., 2015). The MR-PRESSO approach was utilized to identify and exclude SNPs with horizontal pleiotropic outliers, minimizing the impact of pleiotropy on causal estimates (Verbanck et al., 2018). Outliers significant at $p < 0.05$ were removed, and the remaining SNPs were subjected to IVW analysis. The presence of pleiotropy in individual SNPs was determined through the MR-Egger regression intercept, with p-values >0.05 indicating no horizontal pleiotropy (Bowden et al., 2015). Additionally, leave-one-out analysis was conducted to assess the influence of each SNP on pleiotropy.

2.7 Statistical analyses

All analyses were conducted using the Two-Sample MR (Hemani et al., 2018) package in the R environment (ver. 4.3.1; R Development Core Team, Vienna, Austria). Given the exploratory nature of the study. A two-sided p-value that passed the Bonferroni-corrected threshold of 1.22E−04 (0.05/408) was defined as statistically significant. Given the exploratory nature of the study, a p-value <0.05 but above 1.22E−04 was considered suggestive of an association.

3 Results

We conducted a comprehensive MR study utilizing genetically predicted HF trait, LVEF, and NT-pro_BNP to examine their effects on 34 functional gyrus SA and cortical TH, both with and without global weight (global measure as a covariate) (Figure 2). The detailed MR results of the primary analysis, comprising 408 outcomes, are listed in Supplementary Table S7. Additionally, we conducted a subgroup analysis based on SA/TH and identified 18 suggestive associations with various gyri (Figures 3, 4).

Genetically predicted HF trait showed no causal relationship with SA, but was suggested to decrease TH (Figure 3) in the following regions: parsorbitalis without global weighting ($\beta = -$ 2.19e−02 mm, 95% CI: − 3.52e−02 mm to −8.69e−03 mm, $p = 1.18$E−03), lateralorbitofrontal without global weighting ($\beta = -$ 1.69e−02 mm, 95% CI: − 2.93e−02 mm to −4.40e−03 mm, $p = 8.00$E−03), global weighted parsorbitalis ($\beta = -$ 1.38e−02 mm, 95% CI: − 2.53e−02 mm to −2.18e−03 mm, $p = 1.98$E−02), temporalpole without global weighting ($\beta = -$ 2.47e−02 mm, 95% CI: − 4.56e−02 mm to −3.86e−03 mm, $p = 2.02$E−02), lingual without global weighting ($\beta = -$ 1.04e−02 mm, 95% CI: − 1.94e−02 mm to −1.48e−03 mm, $p = 2.24$E−02), and precuneus without global weighting
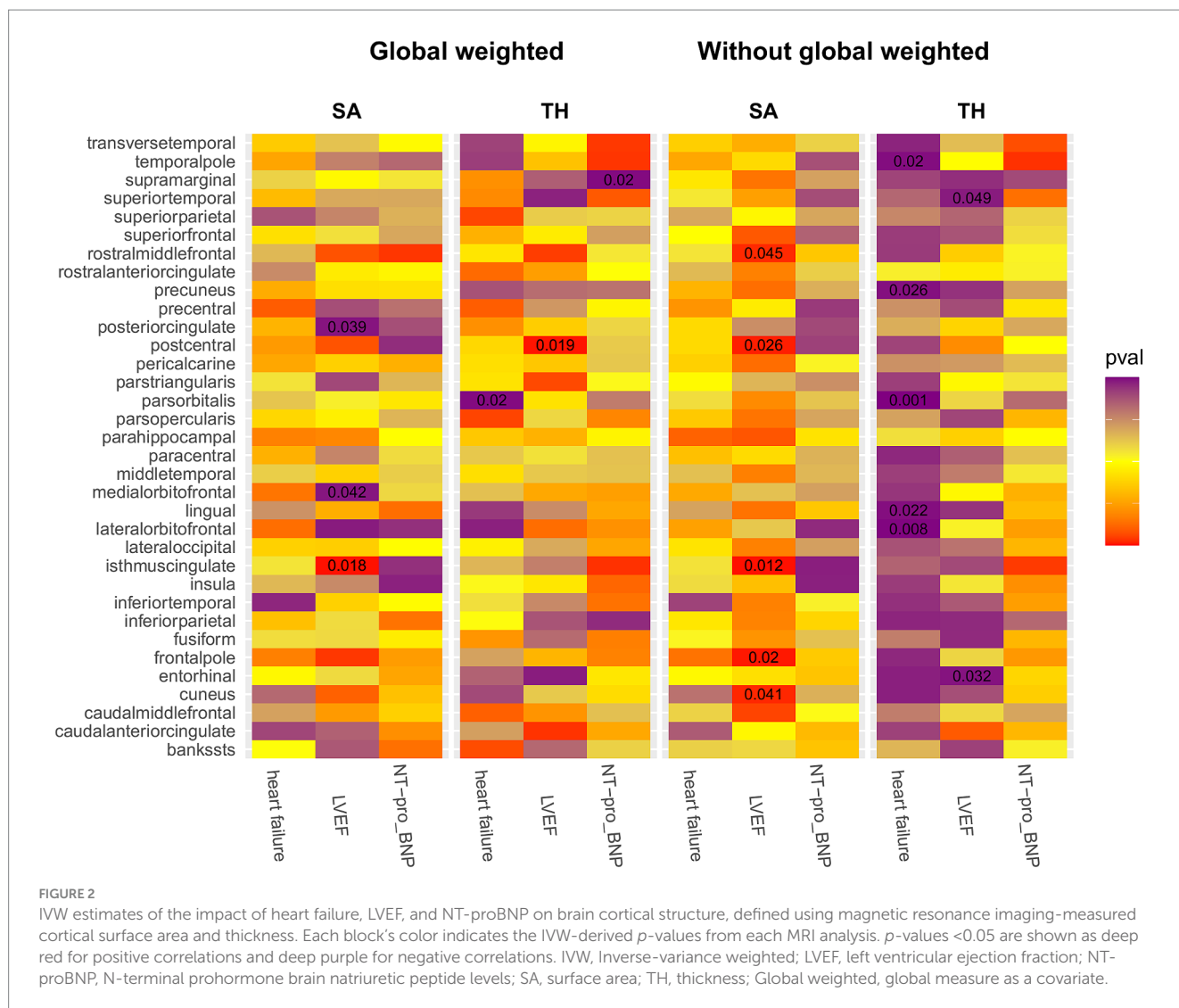
($\beta = -$ 1.31e−02 mm, 95% CI: − 2.46e−02 mm to −1.57e−03 mm, $p = 2.59$E−02). Genetically predicted NT-pro_BNP was suggested to decrease the global weighted supramarginal TH ($\beta = -3.98$e−03 mm, 95% CI: −7.32e−03 mm to −6.33e−04 mm, $p = 1.98$E−02).

Genetically predicted LVEF was suggested to causally increase the SA of six brain regions and the TH of one brain region (Figures 3, 4), as follows: isthmuscingulate SA without global weighting ($\beta = 2.58$ mm², 95% CI: 5.78e−01 mm² to 4.59 mm², $p = 1.15$E−02), global weighted isthmuscingulate SA ($\beta = 1.86$ mm², 95% CI: 3.25e−01 mm² to 3.39 mm², $p = 1.75$E−02), frontalpole SA without global weighting ($\beta = 5.22$e−01 mm², 95% CI: 8.37e−02 mm² to 9.60e−01 mm², $p = 1.96$E−02), postcentral SA without global weighting ($\beta = 6.82$ mm², 95% CI: 8.03e−01 mm² to 12.8 mm², $p = 2.63$E−02), cuneus SA without global weighting ($\beta = 2.65$ mm², 95% CI: 1.14e−01 mm² to 5.19 mm², $p = 4.05$E−02), rostralmiddlefrontal SA without global weighting ($\beta = 9.52$ mm², 95% CI: 2.17e−01 mm² to 18.8 mm², $p = 4.49$E−02), and global weighted postcentral TH ($\beta = 1.52$e−03 mm, 95% CI: 2.48e−04 mm to 2.79e−03 mm, $p = 1.92$E−02). Conversely, it was suggested to negatively correlate with the SA of two brain regions and the TH of two brain regions: global weighted posteriorcingulate SA ($\beta = -1.61$ mm², 95% CI: −3.14 mm² to −8.33e−02 mm², $p = 3.88$E−02), global weighted medialorbitofrontal SA ($\beta = -1.89$ mm², 95% CI: −3.72 mm² to −6.94e−02 mm², $p = 4.19$E−02), entorhinal TH without global weighting ($\beta = -4.87$e−03 mm, 95% CI: −9.32e−03 mm to −4.30e−04 mm, $p = 3.16$E−02), and superiortemporal TH without global weighting ($\beta = -2.60$e−03 mm, 95% CI: −5.18e−03 mm to −1.40e−05 mm, $p = 4.88$E−02).

To ensure the robustness of our findings, we conducted sensitivity analyses using the weighted median and MR-Egger regression methods (Table 1). Notably, the IVW, weighted median, and MR-Egger tests consistently produced results in the same direction. Based on this consistency, we considered the findings to be robust and reliable, and subsequently generated a scatterplot (Supplementary Figures S1−S18). Cochran's Q-derived p-values were all >0.05 (indicating no significant heterogeneity), except for the estimates of heart failure on TH of the lateralorbitofrontal without global weighting and precuneus without global weighting. An outlier (rs4755720) was detected using MR-PRESSO during the estimation of the impact of heart failure on TH of the lateralorbitofrontal without global weighting. Following its exclusion, the analysis was reiterated, and the results were found to be robust, with no significant heterogeneity (IVW: $\beta = -$ 1.37e−02 mm, 95% CI: − 2.46e−02 mm to – 2.70e−03 mm, $p = 1.46$E−02, Cochran's Q derived p-value = 1.58E−01). As we employed random-effects IVW as the primary outcome, a certain degree of heterogeneity was deemed acceptable (Burgess et al., 2019). All p-values (>0.05) derived from the MR-Egger intercept analysis indicated the absence of horizontal pleiotropy. An in-depth scrutiny of our results involved the examination of forest and funnel plots (Supplementary Figures S1−S18). Furthermore, leave-one-out analyses revealed that the estimates were not unduly influenced by any single SNP, further underscoring the robustness of the primary findings.
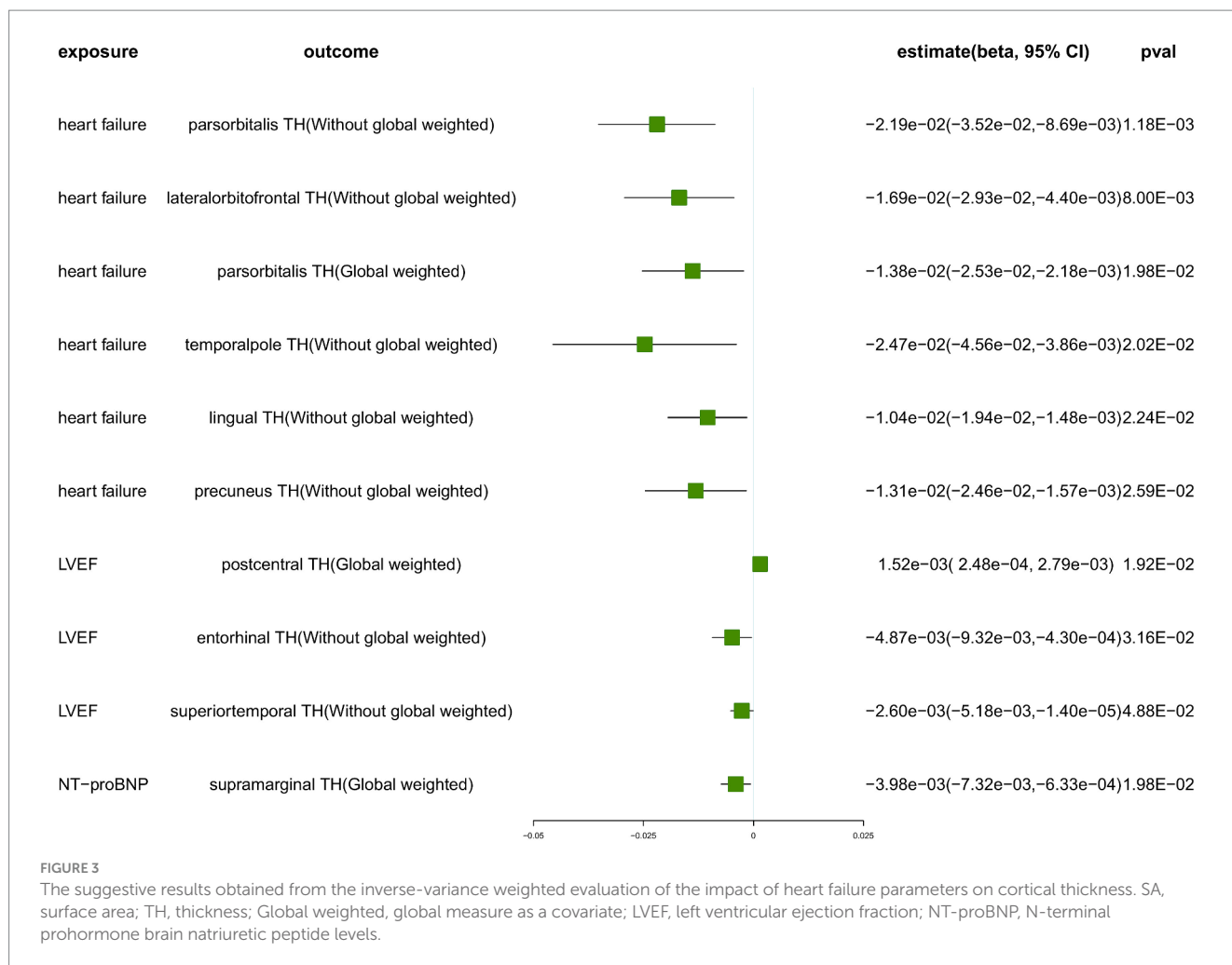
4 Discussion

To investigate the impact of HF on the cortical structure, we conducted a MR analysis from three perspectives of genetically

FIGURE 2
IVW estimates of the impact of heart failure, LVEF, and NT-proBNP on brain cortical structure, defined using magnetic resonance imaging-measured cortical surface area and thickness. Each block's color indicates the IVW-derived *p*-values from each MRI analysis. *p*-values <0.05 are shown as deep red for positive correlations and deep purple for negative correlations. IVW, Inverse-variance weighted; LVEF, left ventricular ejection fraction; NT-proBNP, N-terminal prohormone brain natriuretic peptide levels; SA, surface area; TH, thickness; Global weighted, global measure as a covariate.

predicted HF: HF trait, pathophysiology, and blood biomarkers. Eighteen suggestive associations involving 15 brain regions were identified. Our results found that the HF trait and elevated NT-proBNP were not associated with cortical SA, but were suggestively associated with reduced cortical TH in the pars orbitalis, lateral orbitofrontal cortex, temporal pole, lingual gyrus, precuneus, and supramarginal gyrus. Interestingly, reduced LVEF was primarily suggested to decrease cortical SA in the isthmus cingulate gyrus, frontal pole, postcentral gyrus, cuneus, and rostral middle frontal gyrus, and TH in the postcentral gyrus, but was suggested to increase the SA and TH of certain gyri, including the posterior cingulate gyrus, medial orbitofrontal cortex, entorhinal cortex, and superior temporal gyrus. These brain regions govern higher-order cognitive functions, such as cognition, emotion, perception, memory, and executive control, offering a neuropathological structural basis that elucidates the neurological functional impairments commonly observed in HF patients. Again, these results support the existence of the heart-brain axis and further provide novel insights into its function.

In our study, we found potential structural changes in brain regions associated with cognition and emotion (entorhinal cortex, posterior cingulate gyrus, pars orbitalis, lateral orbitofrontal cortex,

temporal pole, frontal pole, precuneus, supramarginal gyrus, isthmus cingulate gyrus, medial orbitofrontal cortex, and rostral middle frontal gyrus). These changes are believed to be related to the cognitive and emotional impairments observed in patients with HF. Cognitive dysfunction is highly prevalent among individuals with HF, with an estimated 25–75% of patients experiencing some level of impairment (Hajduk et al., 2013; Ampadu and Morley, 2015; Doehner et al., 2018). Past meta-analyses and observational studies have consistently shown that individuals with HF demonstrate an overall decline in cognitive performance and specific deficits in areas such as executive functioning, psychomotor speed, and verbal memory compared to those without a history of HF (Hammond et al., 2018; Connors et al., 2021). Our study further found a potential decrease in cortical TH and SA in brain regions associated with higher cognitive function, which may impair the patients' executive function, verbal memory, and other higher cognitive abilities, consistent with previous research findings. Moreover, neuroimaging studies have revealed that patients with HF exhibit adverse structural brain changes that are associated with cognitive impairment. These include reduced hippocampal volumes (Woo et al., 2015), medial temporal lobe atrophy (Vogels et al., 2007), posterior cingulate cortex atrophy (Almeida et al., 2013), and myelin

exposure	outcome	estimate(beta, 95% CI)	pval
heart failure	parsorbitalis TH(Without global weighted)	−2.19e−02(−3.52e−02,−8.69e−03)	1.18E−03
heart failure	lateralorbitofrontal TH(Without global weighted)	−1.69e−02(−2.93e−02,−4.40e−03)	8.00E−03
heart failure	parsorbitalis TH(Global weighted)	−1.38e−02(−2.53e−02,−2.18e−03)	1.98E−02
heart failure	temporalpole TH(Without global weighted)	−2.47e−02(−4.56e−02,−3.86e−03)	2.02E−02
heart failure	lingual TH(Without global weighted)	−1.04e−02(−1.94e−02,−1.48e−03)	2.24E−02
heart failure	precuneus TH(Without global weighted)	−1.31e−02(−2.46e−02,−1.57e−03)	2.59E−02
LVEF	postcentral TH(Global weighted)	1.52e−03(2.48e−04, 2.79e−03)	1.92E−02
LVEF	entorhinal TH(Without global weighted)	−4.87e−03(−9.32e−03,−4.30e−04)	3.16E−02
LVEF	superiortemporal TH(Without global weighted)	−2.60e−03(−5.18e−03,−1.40e−05)	4.88E−02
NT−proBNP	supramarginal TH(Global weighted)	−3.98e−03(−7.32e−03,−6.33e−04)	1.98E−02

FIGURE 3
The suggestive results obtained from the inverse-variance weighted evaluation of the impact of heart failure parameters on cortical thickness. SA, surface area; TH, thickness; Global weighted, global measure as a covariate; LVEF, left ventricular ejection fraction; NT-proBNP, N-terminal prohormone brain natriuretic peptide levels.
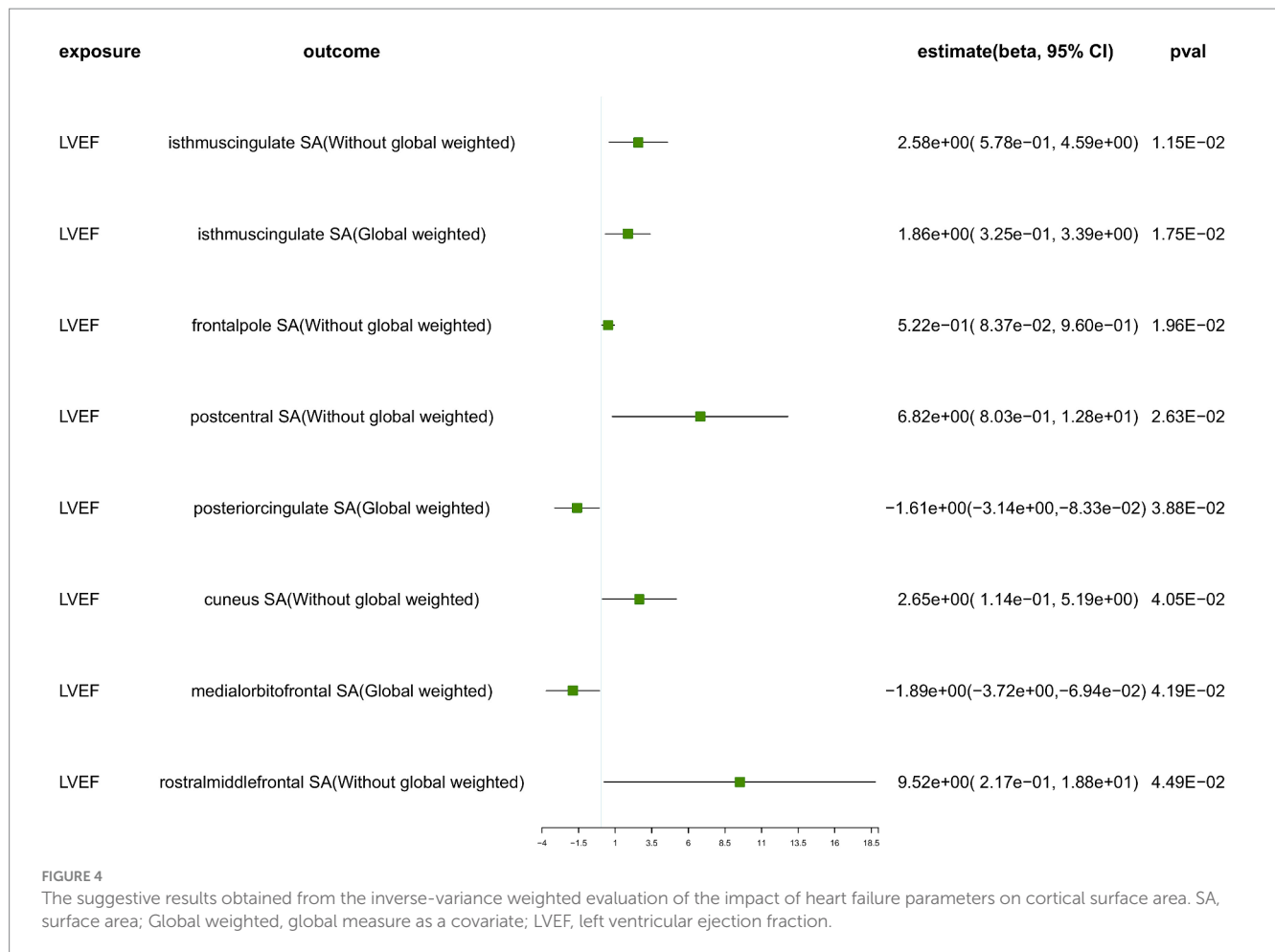
breakdown (Kumar et al., 2011). Additionally, cortical volume reductions have been observed in various lobes, including the frontal (Almeida et al., 2012), temporal (Woo et al., 2003), and parietal (Almeida et al., 2012) lobes, along with an increased white matter lesion burden (Stegmann et al., 2021). The results of these studies are broadly consistent with our findings, but there are also some differences. We did not observe a decrease in cortical TH and SA in the medial temporal lobe. In contrast, we found that a decrease in LVEF was suggestively associated with an increase in cortical TH in the entorhinal cortex, as well as a probable increase in SA in the posterior cingulate gyrus and medial orbitofrontal cortex. In HF patients, the compensatory mechanism of cerebral autoregulation remains intact or even enhanced, and it can compensate for the hypoperfusion caused by HF (Ogoh et al., 2022). This might explain our findings that while a more exquisitely sensitive cortical area undergoes atrophy and volume reduction in the setting of HF, another less vulnerable area might increase in size and volume to temporarily compensate. Further studies are warranted to confirm these findings.

Emotional disorders, particularly depression and anxiety, are commonly observed in patients with HF, with approximately 20–50% experiencing anxiety and 20–45% suffering from depression (Tsabedze et al., 2021; Rashid et al., 2023). Depression is further associated with an increased risk of mortality in this patient population (Sbolli et al., 2020). Studies focusing on brain structural changes in HF patients

with emotional disorders have found an overlap in brain regions associated with emotion and cognition (Woo et al., 2009; Pan et al., 2013; Suzuki et al., 2016). Hippocampal damage is also associated with depression. This association has been confirmed to some extent in animal model experiments (Suzuki et al., 2015). We observed no structural changes in the medial temporal lobe, which includes the hippocampus. This absence of a change may be due to the methodological approach of averaging measurements across both hemispheres, considering that earlier studies have indicated that the right hippocampus is primarily affected by atrophy in HF patients (Woo et al., 2015). Nonetheless, we found potential structural abnormalities in the frontal, temporal, and parietal lobes, particularly in the gyri, that are linked to emotional processing, which supports the results of previous research.

Our study suggested that structural changes in the postcentral gyrus, cuneus, lingual gyrus, and superior temporal gyrus—regions involved in language, sensory processing, and vision—are influenced by HF. Limited research has been conducted on structural brain changes related to speech, sensation, and vision in patients with HF. A study on abnormal autonomic responses to the Valsalva maneuver revealed bilateral damage to the posterior central gyrus, supporting our findings (Song et al., 2018). The absence of gray matter in the cuneus and damage to the lingual gyrus have also been observed in other studies, consistent with our own research findings (Almeida

FIGURE 4
The suggestive results obtained from the inverse-variance weighted evaluation of the impact of heart failure parameters on cortical surface area. SA, surface area; Global weighted, global measure as a covariate; LVEF, left ventricular ejection fraction.

et al., 2012; Park et al., 2016). Contrary to previous research (Almeida et al., 2013), our study found a potential correlation between reduced LVEF and increased TH in the superior temporal gyrus. Further investigation is necessary to validate these findings.

From a mechanistic perspective, HF is associated with reduced cardiac output, inflammatory processes, neurohormoral imbalances, nutritional factors, and damage to brain structures through affected bioelectric and endocrine signaling pathways (Havakuk et al., 2017; Maroofi et al., 2022). These mechanisms are systemic, suggesting that brain damage is widespread rather than confined to specific brain regions. This notion is further supported by our study findings that revealed potential alterations in 15 brain regions.

Advantages of Our Study: First, MR significantly improves traditional methods by addressing confounding factors, reverse causality, and the ethical limitations of randomized controlled trials (RCTs) (Davies et al., 2018). MR uses genetic instruments, specifically, SNPs, which are strongly associated with exposure factors and randomly assorted according to Mendel's second law of inheritance, similar to an RCT (Lawlor et al., 2008). This methodology significantly reduces confounding and robustly assesses causal relationships between exposure and outcome variables (Lawlor et al., 2008). Second, the large sample size in GWAS provides high statistical power, enhancing the robustness and reliability of our findings (Davies et al., 2018). Finally, our study comprehensively examines HF through three aspects: HF trait, LVEF, and NT-proBNP levels. These parameters

represent the clinical phenotype, pathophysiological phenotype, and blood biomarker phenotype of HF, respectively. By incorporating these diverse aspects into an MR analysis of cortical structures, we deepen our understanding of the heart-brain axis.

Our findings not only reveal the potential neuropathological structural changes associated with brain damage caused by HF, but also provide further support for the cognitive, emotional, linguistic, and sensory impairments observed in these patients. Furthermore, our MR analysis fulfilled the assumptions of MR analyses, namely, relevance and independence (Davies et al., 2018). However, this study has several limitations which must be acknowledged. First, owing to the scarcity and heterogeneity of GWAS data on cortical gyral structures, we were unable to validate our current findings using GWAS results from other cortical regions. Second, we discovered inconsistencies between the alterations in the four gyral structures and those reported previously, warranting further research for confirmation. However, the underlying mechanism requires further investigation. Third, we found no significant association between HF and cortical TH or SA (all $p > 1.22E{-}04$). Our findings suggest potential causal relationships, but further studies with larger sample sizes are needed. Finally, it is important to mention that the data was primarily sourced from individuals of European descent. Therefore, additional GWAS studies involving participants from diverse racial backgrounds are necessary to validate the generalizability of our results.

TABLE 1 Suggestive MR estimates from heart failure, Left ventricular ejection fraction and N-terminal prohormone brain natriuretic peptide levels on genetically predicted cortical structure.

Exposure	Outcome	Method	p-val	β (95% Confidence intervals)	Q	Cochran's Q-derived p value	Egger_ intercept	MR-Egger intercept-derived p value
Heart failure	Lateralorbitofrontal TH Without global weighted	Inverse variance weighted	8.00e−03	−1.69e−02 (−2.93e−02, −4.40e−03)	54.77	1.00e−02	4.85e−05	9.61e−01
		MR Egger	4.20e−01	−1.79e−02 (−6.09e−02, 2.51e−02)	54.77	7.34e−03		
		Weighted median	9.27e−02	−1.30e−02 (−2.82e−02, 2.15e−03)				
	Lingual TH Without global weighted	Inverse variance weighted	2.24e−02	−1.04e−02 (−1.94e−02, −1.48e−03)	41.75	1.41e−01	−3.77e−04	5.97e−01
		MR Egger	8.71e−01	−2.53e−03 (−3.29e−02, 2.78e−02)	41.38	1.24e−01		
		Weighted median	4.06e−02	−1.24e−02 (−2.43e−02, −5.32e−04)				
	Parsorbitalis TH Without global weighted	Inverse variance weighted	1.18e−03	−2.19e−02 (−3.52e−02, −8.69e−03)	38.27	2.43e−01	−8.53e−05	9.36e−01
		MR Egger	3.89e−01	−2.02e−02 (−6.54e−02, 2.51e−02)	38.26	2.06e−01		
		Weighted median	7.48e−02	−1.62e−02 (−3.41e−02, 1.62e−03)				
	Precuneus TH Without global weighted	Inverse variance weighted	2.59e−02	−1.31e−02 (−2.46e−02, −1.57e−03)	56.84	6.10e−03	6.60e−05	9.43e−01
		MR Egger	4.76e−01	−1.45e−02 (−5.37e−02, 2.48e−02)	56.83	4.41e−03		
		Weighted median	6.08e−02	−1.32e−02 (−2.70e−02, 6.00e−04)				
	Temporalpole TH Without global weighted	Inverse variance weighted	2.02e−02	−2.47e−02 (−4.56e−02, −3.86e−03)	34.56	3.93e−01	4.27e−04	7.99e−01
		MR Egger	3.63e−01	−3.37e−02 (−1.05e−01, 3.79e−02)	34.48	3.50e−01		
		Weighted median	2.91e−02	−3.41e−02 (−6.48e−02, −3.47e−03)				
	Parsorbitalis TH Global weighted	Inverse variance weighted	1.98e−02	−1.38e−02 (−2.53e−02, −2.18e−03)	44.49	8.74e−02	−2.80e−05	9.76e−01
		MR Egger	5.21e−01	−1.32e−02 (−5.30e−02, 2.66e−02)	44.49	7.01e−02		
		Weighted median	8.83e−02	−1.32e−02 (−2.83e−02, 1.97e−03)				
Left ventricular ejection fraction	Cuneus SA Without global weighted	Inverse variance weighted	4.05e−02	2.65e+00 (1.14e−01, 5.19e+00)	10.59	4.78e−01	7.57e−01	6.83e−01
		MR Egger	8.90e−01	6.88e−01 (−8.85e+00, 1.02e+01)	10.41	4.05e−01		
		Weighted median	2.96e−01	1.83e+00 (−1.60e+00, 5.26e+00)				
	Entorhinal TH Without global weighted	Inverse variance weighted	3.16e−02	−4.87e−03 (−9.32e−03, −4.30e−04)	5.45	9.07e−01	5.83e−05	9.85e−01
		MR Egger	5.60e−01	−5.03e−03 (−2.14e−02, 1.13e−02)	5.45	8.59e−01		
		Weighted median	1.43e−01	−4.31e−03 (−1.01e−02, 1.46e−03)				
	Frontalpole SA Without global weighted	Inverse variance weighted	1.96e−02	5.22e−01 (8.37e−02, 9.60e−01)	8.82	6.39e−01	−5.90e−01	8.13e−02
		MR Egger	3.14e−02	2.06e+00 (4.44e−01, 3.67e+00)	5.06	8.87e−01		
		Weighted median	1.77e−02	7.08e−01 (1.23e−01, 1.29e+00)				

(Continued)

TABLE 1 (Continued)

Exposure	Outcome	Method	p-val	β (95% Confidence intervals)	Q	Cochran's Q-derived p value	Egger_ intercept	MR-Egger intercept-derived p value
	Isthmuscingulate SA Without global weighted	Inverse variance weighted	1.15e−02	2.58e+00 (5.78e−01, 4.59e+00)	7.96	7.17e−01	7.46e−01	6.04e−01
		MR Egger	8.68e−01	6.43e−01 (−6.73e+00, 8.02e+00)	7.67	6.61e−01		
		Weighted median	2.32e−02	3.17e+00 (4.32e−01, 5.90e+00)				
	Postcentral SA Without global weighted	Inverse variance weighted	2.63e−02	6.82e+00 (8.03e−01, 1.28e+01)	8.07	7.07e−01	−3.94e+00	3.68e−01
		MR Egger	1.62e−01	1.71e+01 (−5.09e+00, 3.92e+01)	7.19	7.08e−01		
		Weighted median	1.64e−01	5.87e+00 (−2.39e+00, 1.41e+01)				
	Rostralmiddlefrontal SA Without global weighted	Inverse variance weighted	4.49e−02	9.52e+00 (2.17e−01, 1.88e+01)	5.89	8.80e−01	−8.55e+00	2.16e−01
		MR Egger	9.92e−02	3.17e+01 (−2.49e+00, 6.59e+01)	4.15	9.41e−01		
		Weighted median	1.88e−01	7.96e+00 (−3.88e+00, 1.98e+01)				
	Superiortemporal TH Without global weighted	Inverse variance weighted	4.88e−02	−2.60e−03 (−5.18e−03, −1.40e−05)	16.2	1.34e−01	2.19e−03	2.38e−01
		MR Egger	1.10e−01	−8.31e−03 (−1.76e−02, 9.63e−04)	14	1.73e−01		
		Weighted median	2.46e−01	−1.94e−03 (−5.22e−03, 1.34e−03)				
	Isthmuscingulate SA Global weighted	Inverse variance weighted	1.75e−02	1.86e+00 (3.25e−01, 3.39e+00)	10.86	4.55e−01	2.07e+00	8.04e−02
		MR Egger	2.48e−01	−3.52e+00 (−9.16e+00, 2.11e+00)	7.08	7.18e−01		
		Weighted median	9.93e−02	1.88e+00 (−3.57e−01, 4.13e+00)				
	Medialorbitofrontal SA Global weighted	Inverse variance weighted	4.19e−02	−1.89e+00 (−3.72e+00, −6.94e−02)	10.34	5.00e−01	−5.68e−01	6.66e−01
		MR Egger	9.06e−01	−4.17e−01 (−7.17e+00, 6.34e+00)	10.14	4.29e−01		
		Weighted median	1.40e−01	−1.90e+00 (−4.42e+00, 6.24e−01)				
	Posteriorcingulate SA Global weighted	Inverse variance weighted	3.88e−02	−1.61e+00 (−3.14e+00, −8.33e−02)	5.78	8.88e−01	−6.71e−01	5.42e−01
		MR Egger	9.64e−01	1.32e−01 (−5.50e+00, 5.76e+00)	5.38	8.64e−01		
		Weighted median	9.39e−02	−1.70e+00 (−3.69e+00, 2.89e−01)				
	Postcentral TH Global weighted	Inverse variance weighted	1.92e−02	1.52e−03 (2.48e−04, 2.79e−03)	11.99	3.65e−01	4.21e−04	6.60e−01
		MR Egger	8.75e−01	4.10e−04 (−4.57e−03, 5.39e−03)	11.75	3.02e−01		
		Weighted median	7.24e−02	1.52e−03 (−1.38e−04, 3.17e−03)				
N-terminal prohormone brain natriuretic peptide levels	Supramarginal TH global weighted	Inverse variance weighted	1.98e−02	−3.98e−03 (−7.32e−03, −6.33e−04)	8.38	3.97e−01	2.25e−04	8.06e−01
		MR Egger	2.92e−01	−4.99e−03 (−1.36e−02, 3.59e−03)	8.3	3.07e−01		
		Weighted median	4.51e−02	−4.63e−03 (−9.16e−03, −1.02e−04)				

SA Global weighted, Total Surface Area included as a covariate; TH global weighted, Average Thickness included as a covariate; Without global weighted, without a global measure as a covariate.

5 Conclusion

This is the first comprehensive MR analysis to reveal a potential causal relationship between HF and cortical structures. Overall, we found 15 brain regions likely affected by HF, which may lead to impairments in cognition, emotion, perception, memory, language, sensory processing, vision, and executive control in patients with HF. These findings provide valuable insights into the potential neurological consequences of HF, and further highlight the importance of considering brain health in its management.

Data availability statement

The datasets presented in this study can be found in online repositories. The names of the repository/repositories and accession number(s) can be found at: All data are publicly available. Summary statistics for LVEF and NT-proBNP were obtained from the GWAS Catalog (https://www.ebi.ac.uk/gwas/downloads/summary-statistics) with the identifiers GCST90268125 and GCST90012082, respectively. SNPs data for heart failure were extracted from Rasooly's study (DOI: 10.1038/s41467-023-39253-3). GWAS summary data for cortical structure were downloaded from the ENIGMA consortium website (http://enigma.ini.usc.edu/research/download-enigma-gwas-results). The MR analysis code can be found at https://github.com/shiqinchen/data.

Ethics statement

The studies involving humans were approved by the ethical issues related to the GWAS datasets involved in this study have all been approved by the local ethics committee. The studies were conducted in accordance with the local legislation and institutional requirements. The participants provided their written informed consent to participate in this study.

Author contributions

Funding

Conflict of interest

The authors declare that the research was conducted in the absence of any commercial or financial relationships that could be construed as a potential conflict of interest.

Publisher's note

All claims expressed in this article are solely those of the authors and do not necessarily represent those of their affiliated organizations, or those of the publisher, the editors and the reviewers. Any product that may be evaluated in this article, or claim that may be made by its manufacturer, is not guaranteed or endorsed by the publisher.

Supplementary material

The Supplementary material for this article can be found online at: https://www.frontiersin.org/articles/10.3389/fnins.2024.1416431/full#supplementary-material

References

Almeida, O. P., Garrido, G. J., Beer, C., Lautenschlager, N. T., Arnolda, L., and Flicker, L. (2012). Cognitive and brain changes associated with ischaemic heart disease and heart failure. *Eur. Heart J.* 33, 1769–1776. doi: 10.1093/eurheartj/ehr467

Almeida, O. P., Garrido, G. J., Etherton-Beer, C., Lautenschlager, N. T., Arnolda, L., Alfonso, H., et al. (2013). Brain and mood changes over 2 years in healthy controls and adults with heart failure and ischaemic heart disease. *Eur. J. Heart Fail.* 15, 850–858. doi: 10.1093/eurjhf/hft029

Alosco, M. L., and Hayes, S. M. (2015). Structural brain alterations in heart failure: a review of the literature and implications for risk of Alzheimer's disease. *Heart Fail. Rev.* 20, 561–571. doi: 10.1007/s10741-015-9488-5

Ampadu, J., and Morley, J. E. (2015). Heart failure and cognitive dysfunction. *Int. J. Cardiol.* 178, 12–23. doi: 10.1016/j.ijcard.2014.10.087

Boehm, F. J., and Zhou, X. (2022). Statistical methods for Mendelian randomization in genome-wide association studies: a review. *Comput. Struct. Biotechnol. J.* 20, 2338–2351. doi: 10.1016/j.csbj.2022.05.015

Bowden, J., Davey Smith, G., and Burgess, S. (2015). Mendelian randomization with invalid instruments: effect estimation and bias detection through egger regression. *Int. J. Epidemiol.* 44, 512–525. doi: 10.1093/ije/dyv080

Burgess, S., Davey Smith, G., Davies, N. M., Dudbridge, F., Gill, D., Glymour, M. M., et al. (2019). Guidelines for performing Mendelian randomization investigations: update for summer 2023. *Wellcome Open Res* 4:186. doi: 10.12688/wellcomeopenres.15555.1

Burgess, S., and Thompson, S. G. (2017). Interpreting findings from Mendelian randomization using the MR-egger method. *Eur. J. Epidemiol.* 32, 377–389. doi: 10.1007/s10654-017-0255-x

Connors, E. J., Hauson, A. O., Barlet, B. D., Sarkissians, S., Stelmach, N. P., Walker, A. D., et al. (2021). Neuropsychological assessment and screening in heart failure: a Meta-analysis and systematic review. *Neuropsychol. Rev.* 31, 312–330. doi: 10.1007/s11065-020-09463-3

Davies, N. M., Holmes, M. V., and Davey Smith, G. (2018). Reading Mendelian randomisation studies: a guide, glossary, and checklist for clinicians. *BMJ* 362:k601. doi: 10.1136/bmj.k601

Desikan, R. S., Segonne, F., Fischl, B., Quinn, B. T., Dickerson, B. C., Blacker, D., et al. (2006). An automated labeling system for subdividing the human cerebral cortex on MRI scans into gyral based regions of interest. *NeuroImage* 31, 968–980. doi: 10.1016/j.neuroimage.2006.01.021

Doehner, W., Celutkiene, J., Yilmaz, M. B., and Coats, A. J. S. (2023). Heart failure and the heart-brain axis. *QJM* 116, 897–902. doi: 10.1093/qjmed/hcad179

Doehner, W., Ural, D., Haeusler, K. G., Celutkiene, J., Bestetti, R., Cavusoglu, Y., et al. (2018). Heart and brain interaction in patients with heart failure: overview and proposal for a taxonomy. A position paper from the study group on heart and brain interaction of the heart failure association. *Eur. J. Heart Fail.* 20, 199–215. doi: 10.1002/ejhf.1100

Emdin, C. A., Khera, A. V., and Kathiresan, S. (2017). Mendelian Randomization. *JAMA* 318, 1925–1926. doi: 10.1001/jama.2017.17219

Ference, B. A., Majeed, F., Penumetcha, R., Flack, J. M., and Brook, R. D. (2015). Effect of naturally random allocation to lower low-density lipoprotein cholesterol on the risk of coronary heart disease mediated by polymorphisms in NPC1L1, HMGCR, or both: a 2 x 2 factorial Mendelian randomization study. *J. Am. Coll. Cardiol.* 65, 1552–1561. doi: 10.1016/j.jacc.2015.02.020

Florea, V. G., and Cohn, J. N. (2014). The autonomic nervous system and heart failure. *Circ. Res.* 114, 1815–1826. doi: 10.1161/CIRCRESAHA.114.302589

Folkersen, L., Gustafsson, S., Wang, Q., Hansen, D. H., Hedman, A. K., Schork, A., et al. (2020). Genomic and drug target evaluation of 90 cardiovascular proteins in 30,931 individuals. *Nat. Metab.* 2, 1135–1148. doi: 10.1038/s42255-020-00287-2

Grasby, K. L., Jahanshad, N., Painter, J. N., Colodro-Conde, L., Bralten, J., Hibar, D. P., et al. (2020). The genetic architecture of the human cerebral cortex. *Science* 367:eaay6690. doi: 10.1126/science.aay6690

Greco, M. F., Minelli, C., Sheehan, N. A., and Thompson, J. R. (2015). Detecting pleiotropy in Mendelian randomisation studies with summary data and a continuous outcome. *Stat. Med.* 34, 2926–2940. doi: 10.1002/sim.6522

Hajduk, A. M., Kiefe, C. I., Person, S. D., Gore, J. G., and Saczynski, J. S. (2013). Cognitive change in heart failure: a systematic review. *Circ. Cardiovasc. Qual. Outcomes* 6, 451–460. doi: 10.1161/CIRCOUTCOMES.113.000121

Hammond, C. A., Blades, N. J., Chaudhry, S. I., Dodson, J. A., Longstreth, W. T. Jr., Heckbert, S. R., et al. (2018). Long-term cognitive decline after newly diagnosed heart failure: longitudinal analysis in the CHS (cardiovascular health study). *Circ. Heart Fail.* 11:e004476. doi: 10.1161/CIRCHEARTFAILURE.117.004476

Havakuk, O., King, K. S., Grazette, L., Yoon, A. J., Fong, M., Bregman, N., et al. (2017). Heart failure-induced brain injury. *J. Am. Coll. Cardiol.* 69, 1609–1616. doi: 10.1016/j.jacc.2017.01.022

Hemani, G., Zheng, J., Elsworth, B., Wade, K. H., Haberland, V., Baird, D., et al. (2018). The MR-base platform supports systematic causal inference across the human phenome. *eLife* 7:e34408. doi: 10.7554/eLife.34408

Hooghiemstra, A. M., Leeuwis, A. E., Bertens, A. S., Biessels, G. J., Bots, M. L., Brunner-La Rocca, H. P., et al. (2019). Frequent cognitive impairment in patients with disorders along the heart-brain Axis. *Stroke* 50, 3369–3375. doi: 10.1161/STROKEAHA.119.026031

Kumar, R., Woo, M. A., Macey, P. M., Fonarow, G. C., Hamilton, M. A., and Harper, R. M. (2011). Brain axonal and myelin evaluation in heart failure. *J. Neurol. Sci.* 307, 106–113. doi: 10.1016/j.jns.2011.04.028

Lawlor, D. A., Harbord, R. M., Sterne, J. A., Timpson, N., and Davey Smith, G. (2008). Mendelian randomization: using genes as instruments for making causal inferences in epidemiology. *Stat. Med.* 27, 1133–1163. doi: 10.1002/sim.3034

Li, Y., Guo, J., Cao, Z., and Wu, J. (2022). Causal association between inflammatory bowel disease and psoriasis: a two-sample bidirectional Mendelian randomization study. *Front. Immunol.* 13:916645. doi: 10.3389/fimmu.2022.916645

Maroofi, A., Moro, T., Agrimi, J., and Safari, F. (2022). Cognitive decline in heart failure: biomolecular mechanisms and benefits of exercise. *Biochim. Biophys. Acta Mol. basis Dis.* 1868:166511. doi: 10.1016/j.bbadis.2022.166511

Mueller, K., Thiel, F., Beutner, F., Teren, A., Frisch, S., Ballarini, T., et al. (2020). Brain damage with heart failure: cardiac biomarker alterations and gray matter decline. *Circ. Res.* 126, 750–764. doi: 10.1161/CIRCRESAHA.119.315813

Ogoh, S., Sugawara, J., and Shibata, S. (2022). Does cardiac function affect cerebral blood flow regulation? *J. Clin. Med.* 11:6043. doi: 10.3390/jcm11206043

Pan, A., Kumar, R., Macey, P. M., Fonarow, G. C., Harper, R. M., and Woo, M. A. (2013). Visual assessment of brain magnetic resonance imaging detects injury to cognitive regulatory sites in patients with heart failure. *J. Card. Fail.* 19, 94–100. doi: 10.1016/j.cardfail.2012.12.001

Park, B., Roy, B., Woo, M. A., Palomares, J. A., Fonarow, G. C., Harper, R. M., et al. (2016). Lateralized resting-state functional brain network organization changes in heart failure. *PLoS One* 11:e0155894. doi: 10.1371/journal.pone.0155894

Rashid, S., Qureshi, A. G., Noor, T. A., Yaseen, K., Sheikh, M. A. A., Malik, M., et al. (2023). Anxiety and depression in heart failure: an updated review. *Curr. Probl. Cardiol.* 48:101987. doi: 10.1016/j.cpcardiol.2023.101987

Rasooly, D., Peloso, G. M., Pereira, A. C., Dashti, H., Giambartolomei, C., Wheeler, E., et al. (2023). Genome-wide association analysis and Mendelian randomization proteomics identify drug targets for heart failure. *Nat. Commun.* 14:3826. doi: 10.1038/s41467-023-39253-3

Richmond, R. C., and Davey Smith, G. (2022). Mendelian randomization: concepts and scope. *Cold Spring Harb. Perspect. Med.* 12:a040501. doi: 10.1101/cshperspect.a040501

Sbolli, M., Fiuzat, M., Cani, D., and O'Connor, C. M. (2020). Depression and heart failure: the lonely comorbidity. *Eur. J. Heart Fail.* 22, 2007–2017. doi: 10.1002/ejhf.1865

Schmidt, A. F., Bourfiss, M., Alasiri, A., Puyol-Anton, E., Chopade, S., van Vugt, M., et al. (2023). Druggable proteins influencing cardiac structure and function: implications for heart failure therapies and cancer cardiotoxicity. *Sci. Adv.* 9:eadd4984. doi: 10.1126/sciadv.add4984

Sekula, P., Del Greco, M. F., Pattaro, C., and Kottgen, A. (2016). Mendelian randomization as an approach to assess causality using observational data. *J. Am. Soc. Nephrol.* 27, 3253–3265. doi: 10.1681/ASN.2016010098

Song, X., Roy, B., Fonarow, G. C., Woo, M. A., and Kumar, R. (2018). Brain structural changes associated with aberrant functional responses to the Valsalva maneuver in heart failure. *J. Neurosci. Res.* 96, 1610–1622. doi: 10.1002/jnr.24264

Stegmann, T., Chu, M. L., Witte, V. A., Villringer, A., Kumral, D., Riedel-Heller, S. G., et al. (2021). Heart failure is independently associated with white matter lesions: insights from the population-based LIFE-adult study. *ESC Heart Fail* 8, 697–704. doi: 10.1002/ehf2.13166

Suzuki, H., Matsumoto, Y., Ota, H., Sugimura, K., Takahashi, J., Ito, K., et al. (2016). Hippocampal blood flow abnormality associated with depressive symptoms and cognitive impairment in patients with chronic heart failure. *Circ. J.* 80, 1773–1780. doi: 10.1253/circj.CJ-16-0367

Suzuki, H., Sumiyoshi, A., Matsumoto, Y., Duffy, B. A., Yoshikawa, T., Lythgoe, M. F., et al. (2015). Structural abnormality of the hippocampus associated with depressive symptoms in heart failure rats. *NeuroImage* 105, 84–92. doi: 10.1016/j.neuroimage.2014.10.040

Tsabedze, N., Kinsey, J. H., Mpanya, D., Mogashoa, V., Klug, E., and Manga, P. (2021). The prevalence of depression, stress and anxiety symptoms in patients with chronic heart failure. *Int. J. Ment. Health Syst.* 15:44. doi: 10.1186/s13033-021-00467-x

Verbanck, M., Chen, C. Y., Neale, B., and Do, R. (2018). Detection of widespread horizontal pleiotropy in causal relationships inferred from Mendelian randomization between complex traits and diseases. *Nat. Genet.* 50, 693–698. doi: 10.1038/s41588-018-0099-7

Villringer, A., and Laufs, U. (2021). Heart failure, cognition, and brain damage. *Eur. Heart J.* 42, 1579–1581. doi: 10.1093/eurheartj/ehab061

Vogels, R. L., van der Flier, W. M., van Harten, B., Gouw, A. A., Scheltens, P., Schroeder-Tanka, J. M., et al. (2007). Brain magnetic resonance imaging abnormalities in patients with heart failure. *Eur. J. Heart Fail.* 9, 1003–1009. doi: 10.1016/j.ejheart.2007.07.006

Woo, M. A., Kumar, R., Macey, P. M., Fonarow, G. C., and Harper, R. M. (2009). Brain injury in autonomic, emotional, and cognitive regulatory areas in patients with heart failure. *J. Card. Fail.* 15, 214–223. doi: 10.1016/j.cardfail.2008.10.020

Woo, M. A., Macey, P. M., Fonarow, G. C., Hamilton, M. A., and Harper, R. M. (2003). Regional brain gray matter loss in heart failure. *J. Appl. Physiol.* 95, 677–684. doi: 10.1152/japplphysiol.00101.2003

Woo, M. A., Ogren, J. A., Abouzeid, C. M., Macey, P. M., Sairafian, K. G., Saharan, P. S., et al. (2015). Regional hippocampal damage in heart failure. *Eur. J. Heart Fail.* 17, 494–500. doi: 10.1002/ejhf.241